Energy Use of Ground-Source Heat Pumps for Various Load Temperatures

Nicolas Hache **Guillaume Soudan** **Michel Bernier, PhD, PE**
ASHRAE member

ABSTRACT

This paper examines the impact of the secondary fluid temperatures at the evaporator and condenser on the energy use of water-to-water ground-source heat pumps (GSHP). In the first part of the paper, the energy consumption reduction associated with small temperature differences between source and load temperatures is evaluated from a thermodynamic point-of-view by examining the coefficient of performance (COP) of an ideal refrigeration cycle. Then, the performance map of a typical water-to-water heat pump is examined to determine real COPs for a range of source/load temperatures and flow rates. In the second part of the paper, annual simulations are performed on a ground-source heat pump system providing space heating and domestic hot water (DHW) for a well-insulated single-family house. Two different load temperatures and two different source and load flow rates are examined for a total of eight cases. The concept of seasonal performance factors (SPF) is used to account for all the energy flows into the system including pumping energy. Results show that the highest value of SPF4 (2.44) is obtained when the source and load flow rates are 9.0 gpm (0.56 l/s) and 4.5 gpm (0.28 l/s) respectively, and the return load temperature is 40 °C (104 °F). There is a difference of 8% between the lowest and highest values of SPF4 for the eight cases studied here indicating that the choice of the source and load flow rates as well as the load temperature is relatively important to limit the energy use of GSHP.

INTRODUCTION

Classic thermodynamics tells us that the energy required in a compression heat pump decreases with a reduction of the difference between the condensing and evaporating temperatures of the refrigerant. This can be achieved with efficient heat transfer at the evaporator and condenser and by lowering the difference between the source and load temperatures of the secondary fluids. Recent studies (e.g. Girard et al. 2015, Sarbu and Sebarchievici 2015, and Maivel and Kurnitski 2015) have examined the effects of temperature on heat pump performance. In this study, the impact of the secondary fluid temperatures at the evaporator and condenser on the energy use of water-to-water ground-source heat pumps (GSHP) is examined. In addition, various source and load flow rates of the secondary fluids are examined as they modify heat transfer and refrigerant temperatures in the evaporator and condenser.

This paper is organized as follows. First, the coefficient of performance (*COP*) for an ideal heat pump is presented. Then, *COPs* of a commercially available water-to-water heat pump are reviewed and compared to the *COP* of an ideal heat pump. Finally, seasonal performance factors are calculated based on annual simulations of a GSHP system used for space heating and domestic hot water (DHW) heating of a typical house located in a northern climate.

Nicolas Hache is a graduate student from the Department of Mechanical Engineering, Polytechnique Montreal, Montreal, Canada. Guillaume Soudan is a undergraduate student from the Department of Mechanical Engineering, Polytechnique Mons, Mons, Belgium. Michel Bernier is a professor in the Department of Mechanical Engineering, Polytechnique Montreal, Montreal, Canada.

COP

The four basic components of a heat pump are shown in Figure 1a. The ideal cycle involves an isentropic compression (1-2), a condensation at constant pressure (2-3), an isenthalpic pressure reduction (3-4) and an evaporation at constant pressure (4-1). There is a finite temperature difference between the secondary fluid temperatures, T_{source} and T_{load} , and the refrigerant evaporating and condensing temperatures, T_{evap} and T_{cond} . Hence, the refrigerant temperature in the evaporator is a few degrees lower than the temperature of the secondary fluid on the source side. Similarly, the refrigerant temperature in the condenser is a few degrees higher than the temperature of the secondary fluid on the load side.

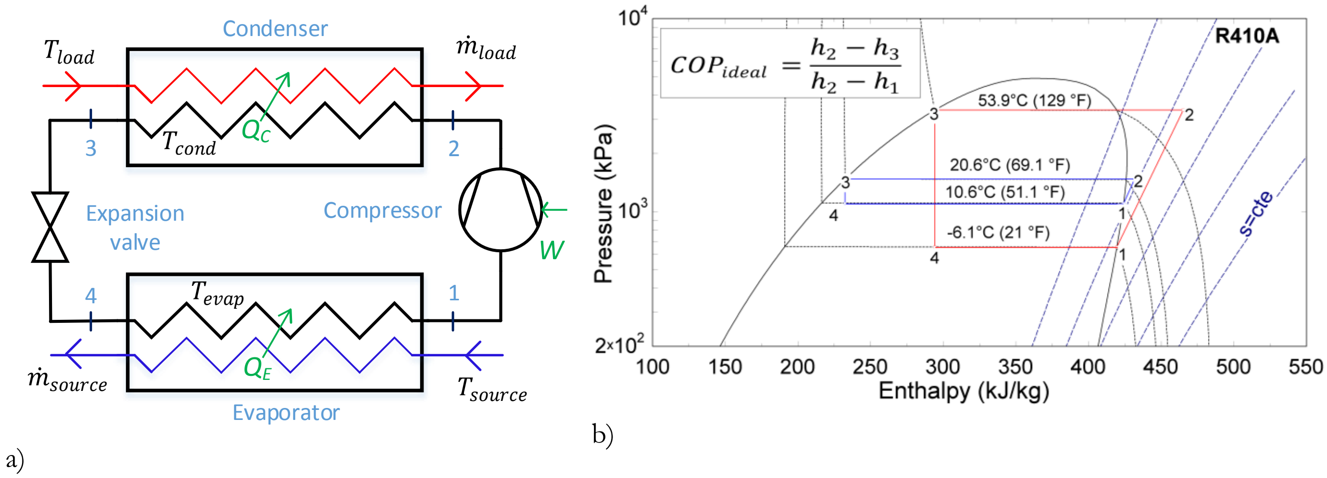

Figure 1 (a) Schematic representation of a compression heat pump and (b) Pressure-enthalpy diagram for two sets of conditions. (1000 kPa = 145 psia ; 300 kJ/kg = 129 Btu/lbm)

Figure 1b shows the P-h diagram for two pairs of (T_{source}/T_{load}), i.e. 30/120 °F (-1.1/48.9 °C) and 60/60 °F (15.6/15.6 °C). The refrigerant used is R-410A and temperature differences (T_{source} - T_{evap}) and (T_{cond} - T_{load}) of 5 K (9 °F) are assumed. The COP_{ideal} values calculated for these conditions are given in Table 1. This table also includes data from a commercially available water-to-water heat pump (used later in this study). The two shaded columns identified by the letter A refer to COP_{ideal}. As shown in this table, COP_{ideal} decreases as the difference between the load and source temperatures increases. The lowest (3.75) and the highest (25.84) values of COP_{ideal} are obtained for source and load temperatures equal to 30/120 °F (-1.1/48.9 °C) and 60/60 °F (15.6/15.6 °C), respectively. This relatively large difference between the lowest and highest values of COP_{ideal} can be explained using the P-h diagram shown in Figure 1b. When the difference between the evaporating and condensing temperatures of the refrigerant is small, the heating effect $(h_2 - h_3)$ is relatively large and the compression work $(h_2 - h_1)$ is relatively small which leads to high values of COP_{ideal}.

In practice, heat pumps do not operate ideally mainly because of compressor inefficiencies. Furthermore, isentropic efficiencies of compressors are not constant but vary as a function of the pressure ratio between the condensing and evaporating temperatures. Thus, the *COP* of a heat pump will not only vary because of the difference between the condensing and evaporating temperatures but also because the compressor efficiency changes with this temperature difference. Actual *COP* values of a commercially available water-to-water heat pump are shown in columns B in Table 1 for four source and four load temperatures as well as two source flow rates and two load flow rates ($\dot{m}_{source}$ and $\dot{m}_{load}$ in Figure 1a). As shown in this table, *COPs* follow the same trend as the values obtained earlier for COP_{ideal} , i.e. they decrease with an increase of the temperature difference (T_{load} -T_{source}). The lowest *COP* value is 2.20 and the highest is 8.60.

High load and source flow rates increase heat transfer coefficients in the evaporator and condenser which reduces the temperature difference (T_{cond} - T_{load}) and (T_{source} -T_{evap}) and increases the value of the *COP*. For example, for a source temperature of -1.1 °C (30 °F) and a load temperature of 48.9 °C (120 °F), the *COP* increases from a value of 2.20 for source and load flow rates both equal to 0.28 L/s (4.5 gpm) to a value of 2.50 when both the load and source flow rates are doubled. Two additional columns representing the ratios of the real *COP* to COP_{ideal} have been added to the right of the B columns. This ratio varies from 0.28 to 0.72 with an average of 0.59. Thus, on average, the *COP* of this heat pump is 59% of COP_{ideal}.

Table 1: Ideal COPs and Performance Data of a Water-to-Water Heat Pump

Source		Load																Source	
			A					B		A					B				
			Flow 4.5 GPM							Flow 9.0 GPM									
EWT (°F)	Flow	EWT (°F)	COP$_{ideal}$	Heating Capacity		Power		COP	COP / COP$_{ideal}$	COP$_{ideal}$	Heating Capacity		Power		COP	COP / COP$_{ideal}$	EWT (°C)	Flow	EWT (°C)
	GPM		-	MBtuh	kW	MBtuh	kW	-	-	-	MBtuh	kW	MBtuh	kW	-	-		l/s	
30	4.5	60	9.54	27.10	7.94	5.25	1.54	5.20	0.55	9.54	27.60	8.09	4.84	1.42	5.70	0.60	15.6	0.28	-1.1
		80	6.57	26.70	7.83	6.72	1.97	4.00	0.61	6.57	27.00	7.91	6.18	1.81	4.40	0.67	26.7		
		100	4.88	26.10	7.65	8.73	2.56	3.00	0.61	4.88	26.00	7.62	8.05	2.36	3.20	0.66	37.8		
		120	3.75	25.10	7.36	11.33	3.32	2.20	0.59	3.75	24.70	7.24	10.44	3.06	2.40	0.64	48.9		
	9	60	9.54	29.20	8.56	5.25	1.54	5.50	0.58	9.54	29.70	8.71	4.84	1.42	6.10	0.64	15.6	0.57	
		80	6.57	28.60	8.38	6.76	1.98	4.20	0.64	6.57	28.90	8.47	6.21	1.82	4.70	0.72	26.7		
		100	4.88	27.70	8.12	8.80	2.58	3.20	0.66	4.88	27.70	8.12	8.09	2.37	3.40	0.70	37.8		
		120	3.75	26.40	7.74	11.40	3.34	2.30	0.61	3.75	26.10	7.65	10.51	3.08	2.50	0.67	48.9		
40	4.5	60	12.25	30.70	9.00	4.81	1.41	6.40	0.52	12.25	31.30	9.17	4.44	1.30	7.10	0.58	15.6	0.28	4.4
		80	7.82	30.60	8.97	6.18	1.81	4.90	0.63	7.82	31.10	9.12	5.70	1.67	5.40	0.69	26.7		
		100	5.59	29.90	8.76	8.15	2.39	3.70	0.66	5.59	30.10	8.82	7.54	2.21	4.00	0.72	37.8		
		120	4.18	28.80	8.44	10.82	3.17	2.70	0.65	4.18	28.60	8.38	9.96	2.92	2.90	0.69	48.9		
	9	60	12.25	34.50	10.11	5.29	1.55	6.50	0.53	12.25	35.20	10.32	4.88	1.43	7.20	0.59	15.6	0.57	
		80	7.82	33.60	9.85	6.79	1.99	4.90	0.63	7.82	34.10	9.99	6.28	1.84	5.40	0.69	26.7		
		100	5.59	32.30	9.47	8.84	2.59	3.70	0.66	5.59	32.50	9.53	8.15	2.39	4.00	0.72	37.8		
		120	4.18	30.70	9.00	11.46	3.36	2.70	0.65	4.18	30.50	8.94	10.54	3.09	2.90	0.69	48.9		
50	4.5	60	16.93	35.90	10.52	5.29	1.55	6.80	0.40	16.93	36.70	10.76	4.88	1.43	7.50	0.44	15.6	0.28	10.0
		80	9.61	35.00	10.26	6.82	2.00	5.10	0.53	9.61	35.60	10.43	6.28	1.84	5.70	0.59	26.7		
		100	6.51	33.80	9.91	8.87	2.60	3.80	0.58	6.51	34.00	9.97	8.15	2.39	4.20	0.65	37.8		
		120	4.71	32.20	9.44	11.46	3.36	2.80	0.59	4.71	32.10	9.41	10.54	3.09	3.00	0.64	48.9		
	9	60	16.93	38.60	11.31	5.32	1.56	7.20	0.43	16.93	39.50	11.58	4.91	1.44	8.00	0.47	15.6	0.57	
		80	9.61	37.50	10.99	6.86	2.01	5.50	0.57	9.61	38.20	11.20	6.31	1.85	6.10	0.63	26.7		
		100	6.51	36.00	10.55	8.90	2.61	4.00	0.61	6.51	36.30	10.64	8.19	2.40	4.40	0.68	37.8		
		120	4.71	34.00	9.97	11.50	3.37	3.00	0.64	4.71	34.00	9.97	10.61	3.11	3.20	0.68	48.9		
60	4.5	60	25.84	39.00	11.43	5.36	1.57	7.30	0.28	25.84	39.90	11.69	4.91	1.44	8.10	0.31	15.6	0.28	15.6
		80	12.36	38.60	11.31	6.86	2.01	5.60	0.45	12.36	39.30	11.52	6.31	1.85	6.20	0.50	26.7		
		100	7.75	37.60	11.02	8.90	2.61	4.20	0.54	7.75	38.00	11.14	8.19	2.40	4.60	0.59	37.8		
		120	5.39	36.00	10.55	11.50	3.37	3.10	0.58	5.39	36.00	10.55	10.61	3.11	3.40	0.63	48.9		
	9	60	25.84	41.50	12.16	5.36	1.57	7.70	0.30	25.84	45.40	13.31	4.95	1.45	8.60	0.33	15.6	0.57	
		80	12.36	41.00	12.02	6.86	2.01	6.00	0.49	12.36	41.80	12.25	6.35	1.86	6.60	0.53	26.7		
		100	7.75	39.80	11.67	8.94	2.62	4.50	0.58	7.75	40.30	11.81	8.22	2.41	4.90	0.63	37.8		
		120	5.39	37.80	11.08	11.53	3.38	3.30	0.61	5.39	45.80	13.42	10.64	3.12	3.60	0.67	48.9		
EWT = Entering Water Temperature			Flow 0.28 l/s							Flow 0.57 l/s									
		Load																	

In summary, the *COP* of a heat pump can be increased by lowering the difference between the secondary fluid temperatures (T_{load} - T_{source}) and by increasing the flow rates of the secondary fluids in both the evaporator and condenser. For a GSHP system operating in heating mode, this implies that the ground heat exchanger length should be as long as possible so that the return temperature to the heat pump is as high as possible. In addition, the load temperature should be as low as possible. Thus, it might be advantageous to couple the heat pump to a low temperature radiant floor instead of using radiators or fan-coils that may require higher operating temperatures. Both source and load flow rates should be as high as possible. The resulting increase in the value of the *COP* can, however, be counterbalanced by increased pumping energy caused by an increase of the pressure drop in the evaporator and condenser and in the rest of the distribution circuits on the source and load sides. The objective of this study is to quantify this impact by determining the energy use of a GSHP system for two load temperatures and two source and load flow rates to determine the best operating scenario.

METHODOLOGY

System Description

The system under study is shown in Figure 2. It consists of a ground-source heat pump providing space heating and domestic hot water (DHW) for a well-insulated single-family house. The energy performance of the system is assessed by running annual simulations using readily available models in TRNSYS v17 (Klein et al. 2010). A time step of 0.1h is used.

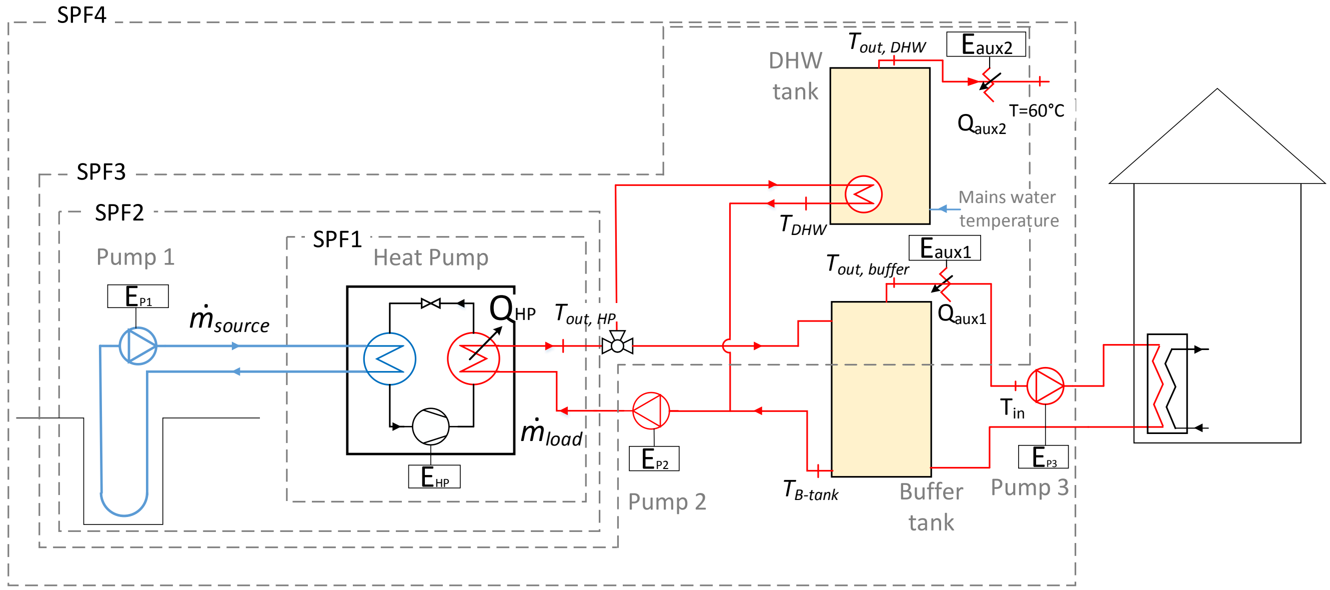

Figure 2 Schematic representation of the system under study.

A 10 kW (3 tons) water-to-water heat pump is connected on the load side to a buffer tank for space heating and to a DHW tank. A 140 m (460 ft.) deep borehole is connected on the source side. A total of three circulating pumps are used (P1, P2, and P3 in Figure 2). A three-way valve is used to divert the flow from one tank to the other with priority given to the buffer tank for space heating. The set-point temperature for the DHW tank is 45 °C (113 °F). Thus, when the return temperature from the DHW tank, T_{DHW}, falls below 45 °C (113 °F) then the heat pump is started along with pumps P1 and P2. Typically, when fully charged, the top temperature in the DHW tank is around 55 °C (131 °F) and a small amount of auxiliary heat is required to reach the desired temperature of 60 °C (140 °F). Space air temperature in the house is controlled with a two-stage thermostat. When the air temperature drops below 21 °C (69.8 °F), pump P3 is activated. If the air temperature continues to drop and reaches 20 °C (68 °F) then an auxiliary heater is energized to supplement the heat from the buffer tank. If pump P3 operates then the temperature of the buffer tank will decrease. If the temperature in the bottom of the buffer tank, $T_{B\text{-}tank}$, reaches a certain set-point then the heat pump as well as pumps P1 and P2 are activated. Two set point temperatures for $T_{B\text{-}tank}$ are examined here: 40 °C (104 °F) and 30 °C (86 °F). The first one may be representative of a system using a fan-coil or radiators while the lower temperature might be associated with a radiant floor heating system. These set point temperatures are constant during the year.

House and DHW Loads

The 220 m² (2350 ft²) house is modeled using TYPE56 in TRNSYS. It is located in a relatively cold climate (Montreal, Canada). The hourly heating load is given in Figure 3a. Peak demand for space heating is approximately 8.7 kW (29.7 kBTU/hr) and the annual space heating requirement is ≈ 20800 kWh (≈ 71 MBTU). As shown in Figure 2, space heating is achieved using a generic heat exchanger. A constant efficiency of 0.9 is assumed in the modeling of this heat exchanger. The daily hot water consumption is 210 liters (55 gallons). The daily draw profile used is the one recommended by Hendron (2008) and it is shown in Figure 3b. The mains water temperature is obtained from the weather processor (TYPE15 in TRNSYS). It varies from 3 °C (37.4 °F) to 15 °C (59 °F) during the year. The annual energy consumption for DHW is approximately 5000 kWh (17.1 MBTU).

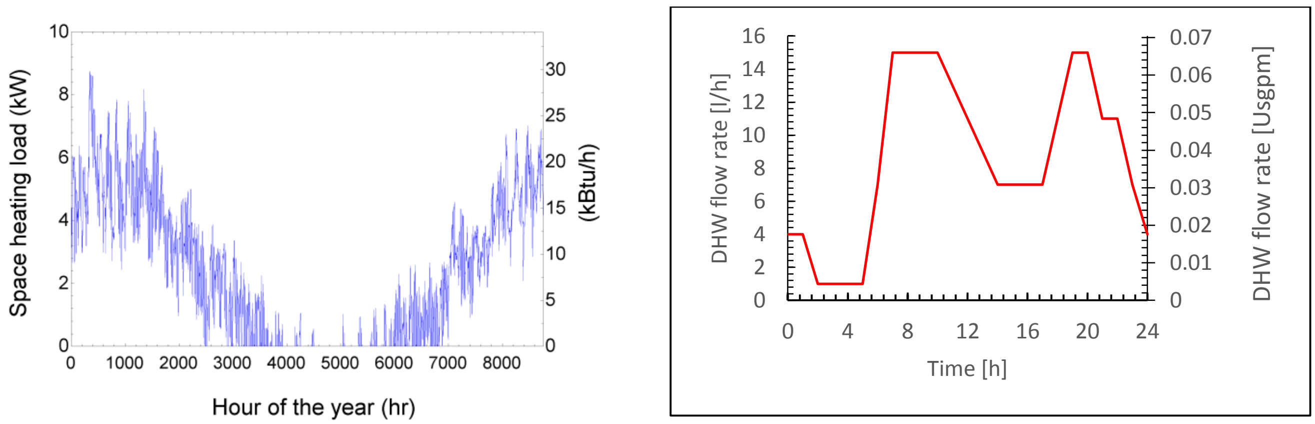

Figure 3 (a) Space heating load and (b) Daily domestic hot water demand.

Models

A borehole model based on the thermal Resistance and Capacitance (RC) approach (Godefroy and Bernier 2014) is used to model the single U-tube borehole. The main characteristics of the borehole are given in Table 2.

Table 2: Main Characteristics of the Borehole

Parameter	Value	Unit	Value	Unit
Depth	140	m	460	ft
Borehole radius	0.075	m	3	in
Outside pipe radius	0.016	m	0.63	in
Borehole thermal resistance	0.1	m.K/W	0.173	h.ft.°F/Btu
Grout conductivity	0.83	W/m.K	0.48	Btu/h.ft.°F
Ground thermal conductivity	2.2	W/m.K	1.27	Btu/h.ft.°F
Pipe conductivity	0.42	W/m.K	0.24	Btu/h.ft.°F
Propylene glycol concentration	25	%	25	%

The heat pump is modeled in TRNSYS as a reversible water-to-water single-stage heat pump (TYPE927). The data presented earlier (see Table 1) is used to represent the performance over the range of source and load temperatures and for the two source and load flow rates.

Table 3: Characteristics of the Circulators

Parameter	Value (low, high) flow rates	Unit	Value (low, high) flow rates	Unit
P1 – Source flow rate	0.28, 0.56	l/s	4.5, 9.0	gpm
Pressure drop in borehole	56, 160	kPa	13.4, 53.5	ft
Pressure drop in heat pump	12, 48	kPa	4, 16	ft
Pump efficiency	15, 30	%	15, 30	%
P2 – Load flow rate	0.28, 0.56	l/s	4.5, 9.0	gpm
Pressure drop in distribution circuit	8, 32	kPa	2.7, 10.7	ft
Pressure drop in heat pump	8, 32	kPa	2.7, 10.7	ft
Pump efficiency	10, 20	%	10, 20	%
P3– Flow rate	0.14, 0.28	l/s	2.25, 4.5	gpm
Pressure drop in distribution circuit	12.5, 50	kPa	4.2 ,16.7	ft
Pump efficiency	10, 15	%	10, 15	%

Circulators are modeled using TYPE741 in TRNSYS. This model calculates the circulator energy consumption for given values of the flow rate, pressure drop, and circulator efficiency. The values of pressure drops and circulator efficiencies assumed here are presented in Table 3. Efficiency ranges from 10 to 30% and depends on the size of the circulator. These values were obtained from a study performed in Europe a dozen years ago (Costic 2003) and may not represent current values in North-America. Therefore, as shown later, these values were doubled to examine the impact of circulator efficiency on the overall results. As noted in Table 3, two flow rates are examined for each pump: 0.28 l/s (4.5 gpm) and 0.56 l/s (9.0 gpm) for P1 and P2; and 0.28 l/s (4.5 gpm) and 0.14 l/s (2.25 gpm) for P3. For P1 and P2, the flow rates correspond to those given in the performance map of the heat pump presented in Table 1. For P3, the two flow rates correspond to cases where $T_{B\text{-}tank}$ are 30 °C (86 °F) and 40 °C (104 °F), respectively.

Both tanks are modeled using TYPE534 in TRNSYS. The volume of the DHW and buffer tanks are 350 liters (92 gallons) and 2000 liters (530 gallons), respectively. Both tanks are insulated and the heat loss coefficient is 0.83 W/m².K (0.15 Btu/h.ft².°F).

RESULTS

A total of eight cases are compared in this section. They are identified by three numbers (a/b/c) where a and b represent the source and load flow rates (in gpm), respectively, and c is the value of $T_{B\text{-}tank}$ (in °C).

Temperatures

Temperature predictions at various locations are presented in Figure 4 for the 9.0/4.5/40 case. The annual variations of the outlet temperature from both tanks as well as the borehole outlet temperature are presented in Figure 4a where simulations start on January 1st. Figure 4b presents a zoomed portion of Figure 4a with the outlet temperature from both tanks and the heat pump. A spline curve fit has been applied to the data in Figure 4a in order to be able to distinguish the top two curves while Figure 4b presents the raw data predicted every 6 minutes.

As shown in Figure 4a, the borehole outlet temperature varies from ≈ -3 (26.6 °F) to ≈ +8 °C (46.4 °F) throughout the year. The minimum value occurs in winter and it increases progressively to a maximum in the summer when the thermal load on the borehole is small due to the intermittent use of the heat pump. As expected, the outlet temperature from the buffer tank is almost constant at 45 °C (113 °F) throughout the year. The outlet temperature from the DHW tank varies from ≈45 (113 °F) to ≈60 °C (140 °F) except in the beginning of the year where there are low temperature occurrences when the space heating load is relatively high and the heat pump supplies heat only to the space heating tank. Figure 4b shows this phenomenon in detail. For example, during the period from t ≈ 415 to 417 hr, the heat pump supplies heat only to the buffer tank at $T_{out,HP}$ ≈ 48 °C (118.4 °F) and $T_{out,DHW}$ decreases from ≈43 °C (109.4 °F) to ≈22 °C (71.6 °F) as cold water temperature enters the DHW tank. At t ≈ 417 hr, space heating needs are satisfied and the heat pump output is directed towards the DHW tank and $T_{out,DHW}$ rises quickly to ≈43 °C (109.4 °F) before the heat pump is switched back to the buffer tank for space heating.

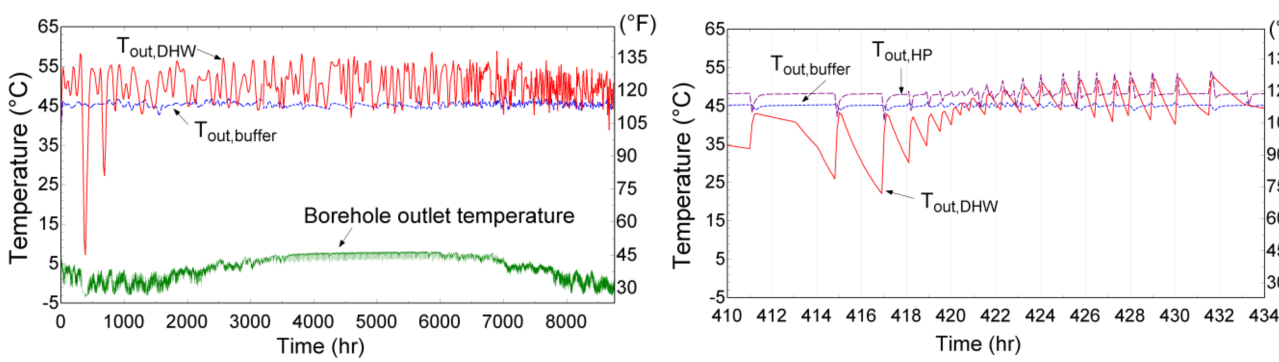

Figure 4 (a) Annual variations of various temperatures (b) Temperature variations for a 24 hour period. Both graphs are for the 9.0/4.5/40 case.

COP and SPF

Typically, values of COP given by manufacturers cover only a few operating points and are usually obtained at full capacity in steady-state conditions. In real installations, these values do not always reflect the real energy performance of heat pumps over entire heating seasons. The concept of seasonal performance factors (SPF) was developed to account for all the energy flows in a heat pump systems and to quantify the energy performance (Nordman and Zottl 2011). This approach was developed in Europe to standardize the representation of heat pump performance based on field measurements and to set common boundaries to evaluate energy flows. Annual simulation results are used here instead of field measurements to obtain SPF values. As shown in Equations 1a to 1d and using the nomenclature of Figure 2, four levels of performance, identified as SPF1 to SPF4, are calculated.

$$SPF1 = \frac{Q_{HP}}{E_{HP}} \quad , \quad SPF2 = \frac{Q_{HP}}{E_{HP} + E_{P1}} \quad , \quad SPF3 = \frac{Q_{HP} + Q_{aux1} + Q_{aux2}}{E_{HP} + E_{P1} + E_{aux1} + E_{aux2}} \quad , \quad SPF4 = \frac{Q_{HP} + Q_{aux1} + Q_{aux2}}{E_{HP} + E_{P1} + E_{P2} + E_{P3} + E_{aux1} + E_{aux2}} \quad \text{(1a, b, c, d)}$$

Values of Q represent annual amounts of heat introduced into the system either from the heat pump, Q_{HP} , or from the two auxiliary heating elements, Q_{aux1} and Q_{aux2}. Values of E represent the annual quantities of energy supplied to each component: E_{HP} for the heat pump, E_{P1}, E_{P2}, E_{P3} for the various circulating pumps, and E_{aux1} and E_{aux2} for the two electric heating elements. It is assumed that the heating elements have an efficiency of 100% and thus $Q_{aux1} = E_{aux1}$ and $Q_{aux2} = E_{aux2}$. The SPF values obtained from annual simulations are presented in Figure 5. The letter "x" above the bar chart shows which case yields the highest value of SPF1, SPF2, SPF3, and SPF4.

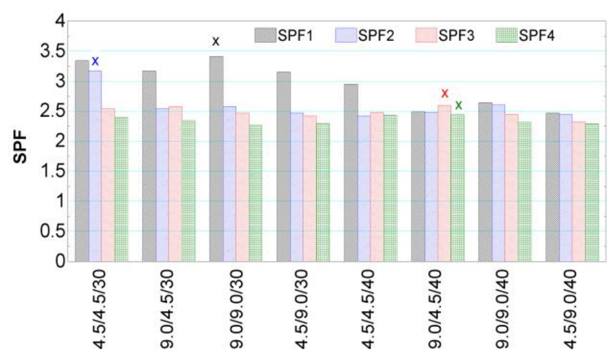

Figure 5 Values of SPF1 to SPF4 for the eight cases studied here.

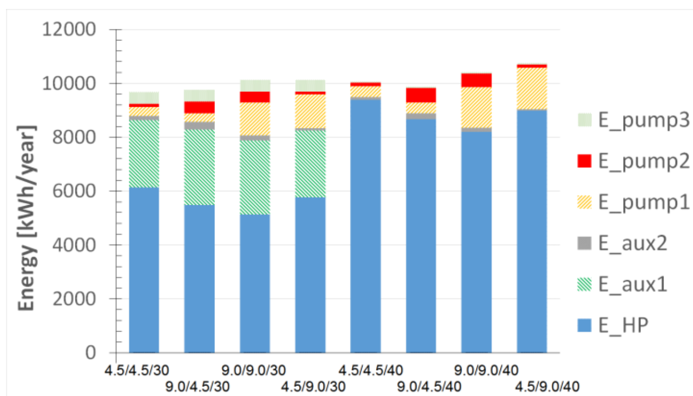

Figure 6 Energy flows for the eight cases studied here. (1000 kWh = 3412 kBtu)

The largest value of SPF1 (3.41) is obtained with the 9.0/9.0/30 combination. This was to be expected as the performance map presented earlier shows that the highest *COP* values are associated with the highest source and load flow rates. However, when the energy requirement of P1 is considered (in SPF2), the SPF1 value of 3.41 drops to 2.58 for SPF2. The largest value of SPF2 (3.17) is obtained with the 4.5/4.5/30 combination. Thus, the increase in *COP* associated with high source and load flow rates is insufficient to counterbalance the increase in the energy consumption of pump P1 when the flow rate is doubled on the source side.

When E_{aux1} and E_{aux2} are considered (in SPF3), the combination 9.0/4.5/40 leads to the highest SPF3 (2.60) followed closely by the 9.0/4.5/30 combination. This is an interesting result as one would have expected to see a much better SPF3 for a $T_{B\text{-}tank}$ of 30 °C (86 °F). These close values of SPF3 can be explained by referring to the energy flows presented in Figure 6. The energy flows are significantly different for the 9.0/4.5/40 and 9.0/4.5/30 cases even though the SPF3 are similar. With a $T_{B\text{-}tank}$ = 30 °C (86 °F), the *COP* of the heat pump is higher but the temperature level is insufficient to completely heat the house and auxiliary heat is required. However, when $T_{B\text{-}tank}$ = 40 °C (104 °F), this temperature level is sufficient to heat the house. In other words, the *COP* is higher for the 9.0/4.5/30 case but a significant portion of heating is performed with a *COP*=1 (electric heating) which in effect reduces the value of SPF3. Finally, as shown in Figure 5, the highest value of SPF4 (2.44) is obtained for the 9.0/4.5/40 combination. There is a difference of 8% between the lowest and highest values of the SPF4.

SPF4 values have also been evaluated by doubling the circulator efficiencies given in Table 3. As shown in Figure 7, the values of SPF4 increase with an increase in circulator efficiency. Numbers over the bars indicate the ranking of each solution. The highest values of SPF4 still occurs for the 9.0/4.5/40 case when circulator efficiency is doubled. However, there are some significant changes to the ranking of the other cases. For example, the ranking for the 4.5/4.5/40 case drops from #2 to #6 when the efficiencies of the circulators is doubled.

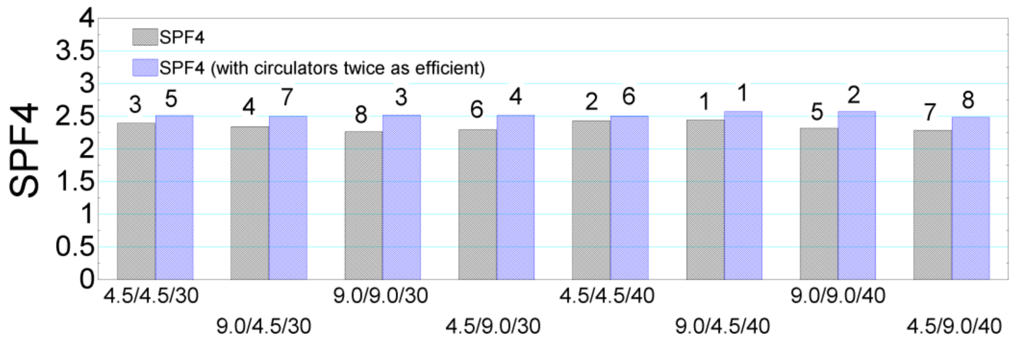

Figure 7 Values of SPF4 with assumed circulators' efficiency and with circulator twice as efficient.

CONCLUSION

This paper examines the impact of various source and load temperatures as well as flow rates on the energy use of water-to-water ground-source heat pumps (GSHP). The *COP* of an ideal refrigeration cycle is first compared to the *COP* of an actual 10 kW (3 tons) heat pump for various conditions. Annual simulations are performed on a ground-source heat pump system providing space heating and domestic hot water (DHW) for a well-insulated single-family house. Two different load temperatures and two different source and load flow rates are examined for a total of eight cases. The concept of seasonal performance factors (SPF) is used to account for all the energy flows into the system including pumping energy. Results show that the highest value of SPF4 (2.44) is obtained when the source and load flow rates are 9.0 gpm (0.56 l/s) and 4.5 gpm (0.28 l/s), respectively, and the return load temperature is 40 °C (104 °F). There is a difference of 8% between the lowest and highest values of SPF4 for the eight cases studied here indicating that the choices of the source and load flow rates as well as the load temperature are relatively important to limit the energy use of GSHP.

REFERENCES

COSTIC. 2003. Rendement des circulateurs selon des données de catalogue. Note 24.013. Février 2003, France.

Girard, A. E.J. Gago, T. Muneer, and G. Caceres. 2015. Higher ground source heat pump COP in a residential building through the use of solar thermal collectors. Renewable Energy, 80:26-39.

Godefroy, V. and M. Bernier. 2014. A simple model to account for thermal capacity in boreholes. Proceedings of the 11th IEA 2014 Heat Pump conference, Montreal (Quebec), Canada, Paper #P.4.8.

Hendron, R. 2008. Building America Research Benchmark definition, updated December 20, 2007. NREL/TP-550-42662.

Klein, S.A. et al, 2010, TRNSYS 17: A Transient System Simulation Program, Solar Energy Laboratory, University of Wisconsin, Madison, USA, http://sel.me.wisc.edu/trnsys.

Maivela, M., and J. Kurnitski. 2015. Heating system return temperature effect on heat pump performance. Energy and Building, 94:71-79.

Nordman, R., and A. Zottl. 2011. SEPEMO-Build-a European project on seasonal performance factor and monitoring for heat pump systems in the building sector. *REHVA Journal*: 56-61.

Sarbu, I., and C. Sebarchievici. 2015. A study of the performances of low-temperature heating systems. Energy Efficiency, 8: 609-627